Acoustic Doppler Velocimetry in Transient Free-Surface Flows: Field and Laboratory Experience with Bores and Surges

Hubert Chanson[1] and Xinqian Leng[2]

Abstract: An understanding of turbulence and mixing is essential to the knowledge of turbulent dissipation, sediment transport, advection of nutrient-rich and organic effluents, and stormwater runoff in prototype water systems, as well as in laboratory channels used for physical modeling of geometrically-scaled full-scale water bodies and for validation of computational models. The acoustic Doppler velocimeter (ADV) system is a robust instrument well suited for such turbulence measurements in open channel flows. The application of acoustic Doppler velocimeter to transient free-surface flows is reviewed in this paper. Based upon field applications and laboratory experiments, the intricacy and inherent difficulties are discussed. The experience and expertise in transient flows highlighted the importance of the signal processing and precise synchronization. Finally, we stress a major benefit of the acoustic Doppler velocimetry for its capability to be used in both field and laboratory, in turn providing some level of confidence in the comparison between full-scale and laboratory data. **DOI: 10.1061/JHEND8.HYENG-14018.**

Author keywords: Turbulence measurements; Acoustic Doppler velocimeter (ADV); Positive surges; Negative surges; Bores; Sediment motion.

Introduction

A fundamental understanding of turbulence and turbulent mixing is essential to the knowledge of turbulent dissipation, sediment transport, advection of nutrient-rich and organic effluents, and stormwater runoff during low flows as well as flood events (Fischer et al. 1979; Rutherford 1994). At prototype scales, the flow motion is turbulent with an unpredictable behavior, a broad spectrum of relevant time and length scales, and strong mixing characteristics (Hinze 1975). Thus, some understanding of turbulence in prototype channels is required, as well as in laboratory channels used for physical modeling of geometrically scaled full-scale systems and for validation of computational models.

Laboratory and field experiences for the past 30 years showed that the ADV system is a robust instrument well suited to turbulence measurements in open channel flows. An acoustic Doppler velocimeter (ADV) is designed to record instantaneous velocity components at a single-point with a relatively high frequency (Kraus et al. 1994). The ADV signal strength may provide further information on the instantaneous suspended sediment concentration (SSC), although the implementation requires a proper calibration (Fugate and Friedrichs 2002; Chanson et al. 2008). To date, the vast majority of applications covered steady free-surface and periodic flow conditions (Lohrmann et al. 1994; Voulgaris and Trowbridge 1998; Nikora and Goring 2000; Mori et al. 2007).

In this contribution, the application of acoustic Doppler velocimeter to transient free-surface flows is reviewed. Present experience suggests that some main advantages of using acoustic Doppler velocimetry in transient free-surface flow include the high sampling frequency (up to 200 Hz), the relative ease to synchronization with other instruments, and the ability to use the same instrumentation (i.e., ADV) in the field and in the laboratory. Based upon field applications and laboratory experiments, the intricacy and inherent difficulties are discussed. A number of signal processing techniques are illustrated and best practices are documented.

Basic Principles of ADV Metrology

An acoustic Doppler velocimeter (ADV) enables remote two- or three-dimensional velocity measurements in water flows at relatively high sampling rates in a small sample volume. The instrument was originally developed for use in laboratory (Kraus et al. 1994). Field deployments have since demonstrated its robustness, e.g., under 3 m high breaking waves (Lohrmann et al. 1995) and in tidal bores in large river (Chanson et al. 2007; Keevil et al. 2015; Reungoat et al. 2018). The ADV operates using the Doppler shift principle. Short acoustic pulses are emitted along the transmit beam. The phase data reflected by small particles from successive coherent acoustic returns are detected by the receivers and converted into velocity estimates using a pulse-pair processing technique (Kraus et al. 1994; Voulgaris and Trowbridge 1998; Mclelland and Nicholas 2000). Implicitly, the acoustic Doppler velocimetry requires a minimum of particles in the water.

A typical acoustic Doppler velocimeter (ADV) is equipped with n receivers (Fig. 1) which simultaneously acquire $4 \times n$ parameters at each sample: a velocity component, signal strength, signal-to-noise ratio (SNR) and correlation. The last three parameters are typically used to ascertain the signal quality and accuracy of velocity data, although the signal strength can be linked to the instantaneous suspended sediment concentration in the control volume

[1]Professor, Hydraulic Engineering, School of Civil Engineering, Univ. of Queensland, Brisbane, QLD 4072, Australia (corresponding author). ORCID: https://orcid.org/0000-0002-2016-9650. Email: h.chanson@uq.edu.au

[2]Honorary Lecturer, School of Civil Engineering, Univ. of Queensland, Brisbane, QLD 4072, Australia. Email: xinqian.leng@uqconnect.edu.au

Note. This manuscript was submitted on November 28, 2023; approved on April 22, 2024; published online on July 10, 2024. Discussion period open until December 10, 2024; separate discussions must be submitted for individual papers. This paper is part of the ***Journal of Hydraulic Engineering***, © ASCE, ISSN 0733-9429.

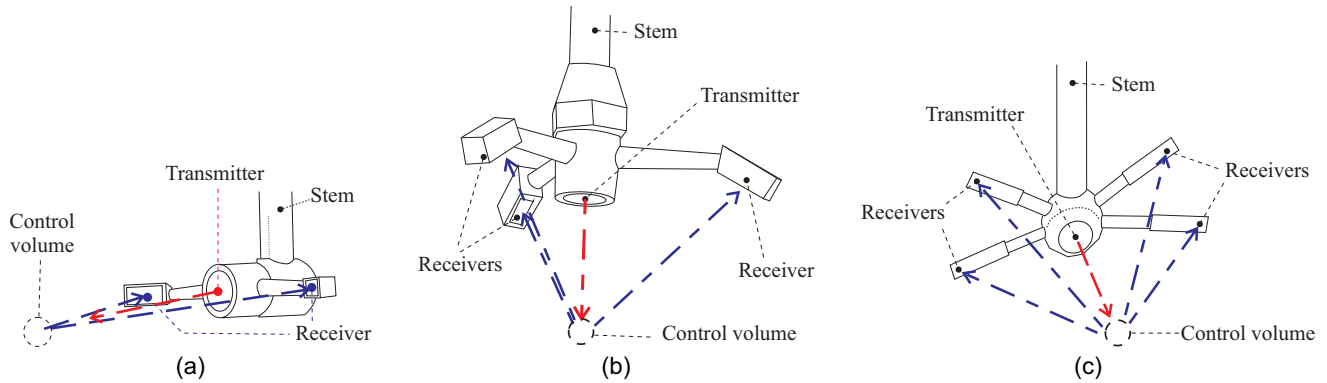

Fig. 1. Acoustic Doppler velocimeter(s) with two, three and four receivers: (a) two receivers ($n = 2$) side-looking head; (b) three receivers ($n = 3$) down-looking head; and (c) four receivers ($n = 4$) side-looking head.

(Fugate and Friedrichs 2002; Chanson et al. 2008; Salehi and Strom 2011). The velocity data is measured along the line connecting the sampling volume to the receiver (Fig. 1), before being transformed into a Cartesian system of coordinates.

The ADV signal output includes the combined effects of turbulent velocity fluctuations, Doppler noise, signal aliasing, turbulent shear, installation vibrations and other disturbances (e.g., navigation, fish activity). The signal may be further affected adversely by velocity shear across the sampling volume and boundary proximity (Finelli et al. 1999; Liu et al. 2002; Chanson et al. 2007). Plainly, the raw ADV velocity signal does not represent the true turbulent velocities and should never be used without adequate postprocessing (Nikora and Goring 1998; Goring and Nikora 2002; Wahl 2003).

Experience in Transient Free-Surface Flow Measurements

Some comprehensive unsteady flow measurements were performed in transient surges during the past decades (e.g., Hornung et al. 1995; Koch and Chanson 2008; Wűthrich et al. 2016; Thomas and David 2022). A number of signal analysis methods were tested, including single experiment, Fourier component method, ensemble averaging and ensemble statistics of Fourier component analyses (Chanson 2020). Tables 1 and 2 list several such studies using acoustic Doppler velocimetry. Some key outcomes derive from the laboratory and field measurement experiences and associated signal output analyses. A single run or single realization without additional signal analysis delivers a combination of qualitative observations and instantaneous signal quantities. This approach is not suitable to obtain accurate quantitative turbulence data in transient free-surface flows such as the leading edge of dam break waves, surges and bores, in which the relevant time scales of hydrodynamic processes are less than a second, i.e., often between 0.2 s and 0.5 s at the full-scale [Figs. 2(a and b)]. The Fourier component analysis is based upon a band-pass filtering of the velocity signal, and sometimes referred to as variable interval time average (VITA) technique. The approach is reasonably well-suited to transient free-surface flows, and was successfully applied to laboratory experiments and field measurements (Tables 1 and 2). The instantaneous time-series, e.g., of the velocity signal V, may be represented as a superposition of two components:

$$V = \langle V \rangle + \{V\} \quad (1)$$

where <V> the low-pass filtered contribution, and {V} is the high-pass filtered component corresponding to the turbulent fluctuation. The application of the Fourier component analysis relies upon the selection of a physically meaningful threshold frequency F_c, much smaller than the instrument sampling frequency, and the analyzed outputs must not be overly sensitive to the precise selection of the threshold frequency F_c (Chanson and Docherty 2012; Aleixo et al. 2019). Fig. 3 illustrates the application of Fourier component analysis to some field data, in the transient bore seen in Fig. 2(b).

When the measurements can be repeated in laboratory [Figs. 2(c and d)], the ensemble statistics is a most reliable methodology (Bradshaw 1971). The successful implementation of ensemble averaging was conducted in compression waves and expansion waves (Table 1 and 2). The repetitions of the experiment necessitate some great care to ensure the repeatability of the physical process as well as the synchronization between repeated experimental runs. These issues are critical and not simple to solve, despite too few mentions in the literature (Leng et al. 2018b). When experiments simultaneously record several instruments, the synchronization of all recording systems can be done mechanically, electrically, or electronically. With transient free-surface flows, the synchronization between different repeats should be based upon the disturbance generation time, e.g., gate opening for a dam break wave, gate closure for a breaking bore generation. Chanson and Docherty (2012) further tested the application of the Fourier component analysis averaged over 20 experimental runs in positive surges. The results showed comparable outcomes with the ensemble averaging performed over 20 runs, despite the more cumbersome computational time.

With any ensemble statistical analyses, a minimum number of repetitions is essential to ensure the data quality and accuracy. The traditional approach in free-surface wave motion and dam break wave is to perform a small number of repeats, i.e., three to five (Hornung et al. 1995; Aleixo et al. 2019; Rajaie et al. 2022). In the authors' opinion, this small number of repeats is insufficient to derive turbulence characteristics (Chanson 2020). A number of sensitivity analyses were performed (Leng and Chanson 2015, 2016, 2017a). In free-surface flows, the data were basically independent of the number of realizations in terms of free-surface properties, longitudinal velocity and average tangential Reynolds stress for a minimum of 20 runs. Practically, the selection of 25 repetitions is consistent with earlier turbulence literature (Perry et al. 1980) and provides a reasonable compromise between accuracy and resources (Chanson 2020). Importantly, it must be stressed that the selection of the flow property has a major influence on the

Table 1. Acoustic Doppler velocimeter (ADV) measurements in transient free-surface flows in fixed boundary channels

References	Transient flow motion	ADV	Signal sampling and processing	Initial water depth d_o (m)	Initial water velocity V_o (m/s)	Surge celerity U (m/s)	Comment
Reichstetter (2011)	Negative surge	Nortek Vectrino+ (10 MHz)	200 Hz (continuous), Fourier component method	0.24	0.17	0.91	Laboratory channel (L = 12 m, B = 0.5 m)
Leng and Chanson (2015)	Negative surge	Nortek Vectrino+ (10 MHz)	200 Hz (continuous), Ensemble-averaging (25 runs minimum)	0.11–0.23	0.22–0.45	0.5–1.25	Laboratory channel (L = 12 m, B = 0.5 m)
Koch and Chanson (2008)	Positive surge	Sontek MicroADV (16 MHz)	50 Hz (continuous), Fourier component method	0.079	1.0	0.235 0.54	Laboratory channel (L = 12 m, B = 0.5 m)
Chanson and Docherty (2012)	Positive surge	Nortek Vectrino+ (10 MHz)	200 Hz (continuous), Fourier component method, Ensemble-averaging (20 runs), Fourier component method (20 runs)	0.117 0.126	0.85 0.79	0.87 0.86	Laboratory channel (L = 12 m, B = 0.5 m)
Leng and Chanson (2017b)	Positive surge	Nortek Vectrino+ (10 MHz)	200 Hz (continuous), Ensemble-averaging (25 and 50 runs)				Laboratory channel (L = 17 m, B = 0.7 m)
Leng and Chanson (2017a)	Positive surge	Nortek Vectrino II profiler	100 Hz (continuous), Ensemble-averaging (25 and 50 runs)	0.177	0.79	1.29	Laboratory channel (L = 17 m, B = 0.7 m)
Leng and Chanson (2018)	Positive surge	Array of two Nortek Vectrino II profilers	100 Hz (continuous), Ensemble-averaging (25 runs)	0.174 0.176 0.176	0.83 0.82 0.82	1.15 1.11 1.18	Laboratory channel (L = 17 m, B = 0.7 m)

Note: B: channel width; d_o: initial average water depth; L: channel length; U: surge celerity positive upstream; and V_o: initial streamwise velocity positive downstream.

04024034-3

Table 2. Acoustic Doppler velocimeter (ADV) measurements in transient free-surface flows in mobile bed channels

Reference	Transient flow motion	ADV	Signal sampling and processing	Initial water depth d_o (m)	Initial water velocity V_o (m/s)	Surge celerity U (m/s)	Sediment	Comment
Chanson et al. (2011)	Positive surge	Nortek Vector (6 MHz)	64 Hz (continuous), Fourier component method	1.43	0.30	4.2	Fine mud and silt	Tidal bore of Garonne River at Arcins on 11 Sept. 2010
Furgerot et al. (2013)	Positive surge	Nortek Vector (6 MHz)	64 Hz (continuous)	0.9	0.3	3.2	Mixed sediments ("tangue")	Tidal bore of Sée River at Le Bateau on 7 May 2012
Keevil et al. (2015)	Positive surge	Nortek Vectrino+ (10 MHz)	200 Hz (continuous), Fourier component method	1.32	0.26	4.75	Fine mud and silt	Tidal bore of Garonne River at Arcins on 19 Oct. 2013
Leng et al. (2018a)	Positive surge	Nortek Vectrino+ (10 MHz)	200 Hz (continuous), Fourier component method, Turbulent event threshold technique	1.685 1.12 1.24	0.29 0.18 0.22	4.23 1.79 4.61	Fine mud and silt	Tidal bore of Garonne River at Arcins on 29 and 31 Aug. 2015 ad 27 Oct. 2015
Khezri and Chanson (2012)	Positive surge	Nortek Vectrino+ (10 MHz)	200 Hz (continuous), Fourier component method	0.136	0.74	0.61 0.87	Natural gravel (4.75 < Ø < 6.7 mm)	Laboratory channel (L = 12 m, B = 0.5 m)
Li (2020)	Positive surge	Nortek Vectrino+ (10 MHz)	200 Hz (continuous), Ensemble-averaging (25 runs minimum)	0.106 0.124 0.174	0.74 0.98 0.70	0.34 0.92 1.12	Natural gravel (6. 7 < Ø < 9.5 mm)	Laboratory channel (L = 15 m, B = 0.5 m)
Zhang et al. (2022)	Positive surge	Nortek Vectrino+ (10 MHz)	200 Hz (continuous)	0.03-0.07	—	—	Sand (Ø = 2 mm)	Laboratory channel (B = 2 m)
Rajaie et al. (2022)	Positive surge	Nortek Vectrino+ (10 MHz)	200 Hz (continuous), Ensemble-averaging (3 runs)	0.25-0.4	0	—	Sand (Ø = 0 mm)	Laboratory channel (L = 30 m, B = 1.5 m)

Note: B: channel width; d_o: initial average water depth; L: channel length; U: surge celerity positive upstream; V_o: initial streamwise velocity positive downstream; and (—): data not available.

J. Hydraul. Eng.

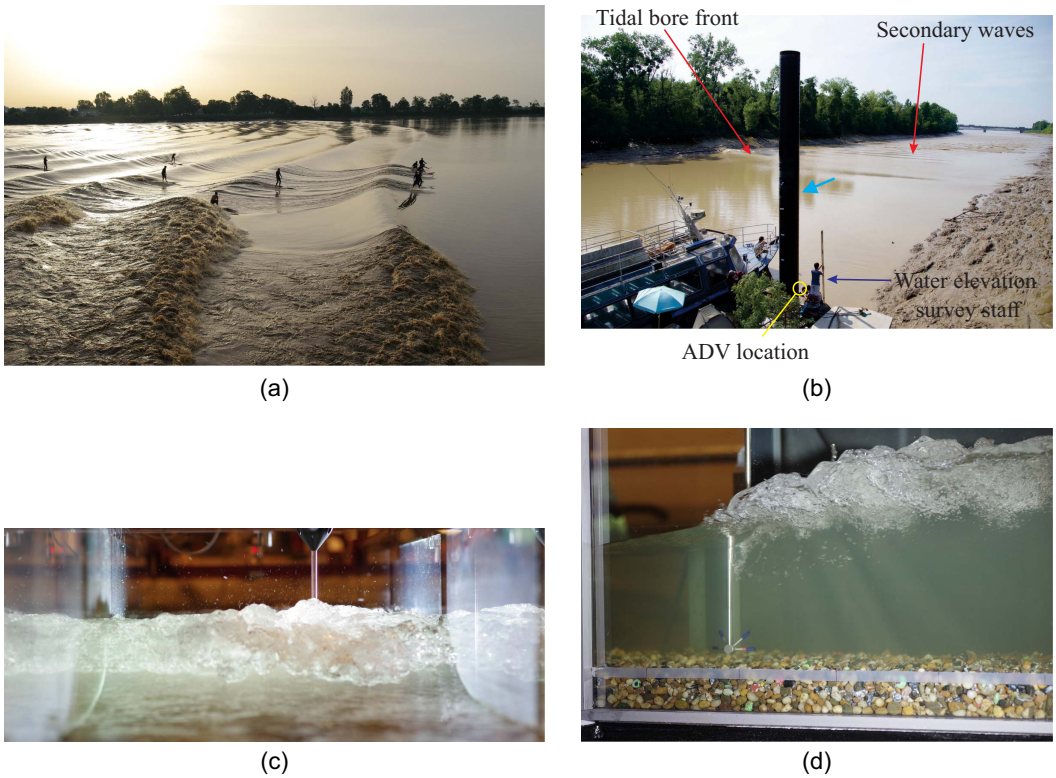

Fig. 2. Transient free-surface flows at full-scale and in laboratory: (a) tidal bore of the Dordogne River at St Pardon (France) at sunrise on 17 June 2022 with bore propagation from left to right against the fluvial motion; (b) field measurement using acoustic Doppler velocimetry in the Garonne River tidal bore at Arcins (France); (c) front view of positive surge on mobile bed in laboratory— Flow conditions: Fr = 1.6, d_o = 0.131 m, U = 0.97 m/s, B = 0.5 m—Looking downstream at the incoming surge advancing upstream toward the camera (shutter speed: 1/250 s) with an acoustic Doppler velocimeter Nortek^{TM} Vectrino+ on the right. (Images by Hubert Chanson.); and (d) side view of positive surge on mobile bed in laboratory— Flow conditions: Fr = 1.6, d_o = 0.131 m, U = 0.97 m/s, B = 0.5 m = Sideview of bore front over mobile bed (shutter speed: 1/250 s) with an acoustic Doppler velocimeter Nortek^{TM} Vectrino+—Bore propagation from right to left—Note the side-looking head with four receivers.

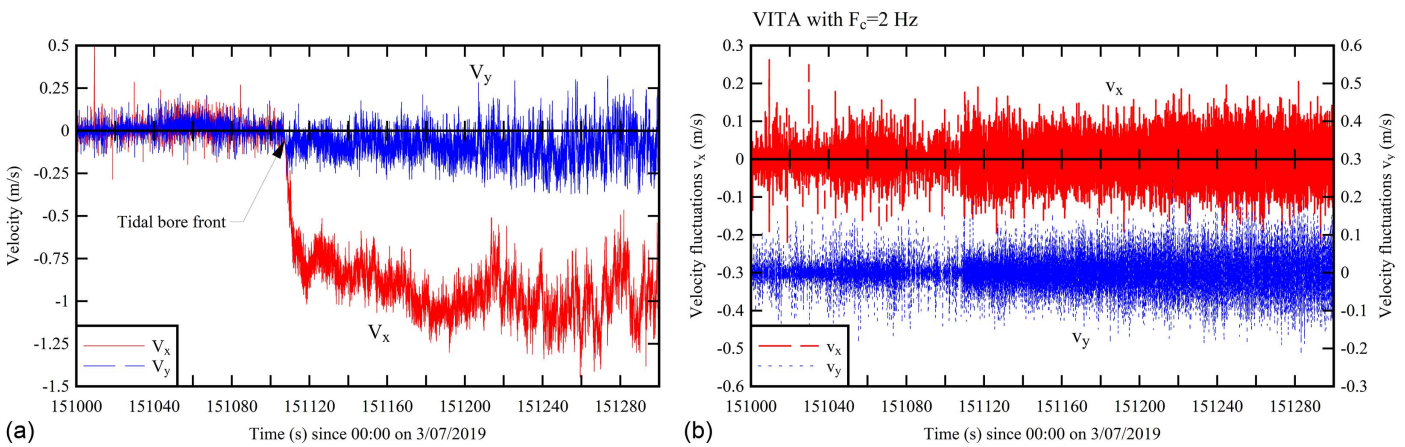

Fig. 3. Application of Fourier component analysis to ADV measurements in the Garonne River tidal bore at Arcins (France) on 4 July 2019 afternoon-F_c = 2 Hz, tidal bore front passage at t = 151,107 s-Flow conditions: d_o = 0.57 m, U = 3.85 m/s, ADV sampling rate: 200 Hz (continuous): (a) instantaneous longitudinal and transverse velocity data, V_x and V_y respectively; and (b) instantaneous longitudinal and transverse velocity fluctuations, v_x and v_y respectively.

sensitivity analysis outcomes, e.g., with different results in terms of mean velocity, velocity fluctuation, turbulent Reynolds stress, or integral turbulent scales (Leng and Chanson 2015, 2017a). The experience suggests that a larger number of experimental repetitions is necessary for advanced flow properties, such as triple correlations, extreme pressure data or air-water flow properties. Ultimately, the number of repeats cannot match the number of data samples used in seminal steady turbulent flow analysis

(Karlsson and Johansson 1986; Krogstad et al. 2005). Practically, the repeatability of the experiment and the quality of synchronization between repeats are uppermost important, possibly much more relevant than the number of repeats, on the quality and accuracy of the results in transient free-surface flows. Furthermore, in transient free-surface flows, the ensemble data must be statistically analyzed in terms of robust estimators which are little sensitive to outliers, e.g., instantaneous median, quartiles and percentiles. A complete data analysis may be extended to unsteady turbulent burst detections (Leng et al. 2018a; Shi et al. 2020).

Up to date, a limited number of transient flow studies were successfully conducted based upon experimental ensemble statistics, e.g., Chanson and Docherty (2012), Leng and Chanson (2016, 2017a, b), and Wang et al. (2017) (also Table 1), often because of practical technical limitations, time constraints and limited resources. While an ensemble approach is the best methodology in laboratory under well-controlled experimental conditions, field measurements in transient flows are unlikely to be repeatable in most situations. A Fourier component may therefore be the most appropriate statistical analysis, as shown by the field observations in the tidal bores of the Garonne and Sélune Rivers (Mouaze et al. 2010; Keevil et al. 2015; Reungoat et al. 2018).

Finally, the two authors developed an extensive experience in the use of ADV systems in laboratories and in the field, in estuaries and in rivers, with both (quasi-)steady and unsteady transient flow conditions. In the case of transient free-surface flows, they used the same ADV Nortek Vectrino+ system in both field and laboratory, e.g., Leng and Chanson (2015, 2016), and Reungoat et al. (2017). Leng et al. (2018a), while the first author used some ADV Sontek microADV and ADV Nortek Vector units in both situations (Chanson et al. 2011; Mouaze et al. 2010). In the case of the Nortek Vector and Sontek microADV, the units were exactly identical between laboratory and field. With the Nortek Vectrino+, an ADV Field stem and head was used instead in the field. The experience suggested that the only difference between laboratory and field applications was the power settings of the ADV units. In laboratory, the power setting was set to maximum because of the low particle counts, while a lower power setting had to be applied in the field, because the very large number of suspended particles [and adverse impact on velocity signal, e.g., Chanson et al. (2010)].

Transient Free-Surface Flows and Sediment Motion

In transient free-surface flows, very high short-lived turbulence is observed beneath the leading edge of the disturbance and in its wake (Spinewine 2005; Reichstetter 2011; Leng 2018). The large turbulent stresses are conducive to the transport and advection of sediments, including bed load motion, sheet flows, and sediment suspension (Nielsen 1992; Halfi et al. 2020, 2023). Thus, the acoustic Doppler velocimetry is a suitable technique to characterize the unsteady turbulence, while the ADV signal amplitude may be used as a proxy for suspended sediment concentration with proper calibration (Table 2).

In laboratory, two studies simultaneously performed acoustic Doppler velocity measurements and video recordings of sediment inception and transient sediment motion under positive surges (Khezri and Chanson 2012; Li 2020) (Table 2). Both experiments used an ensemble-statistical approach, with a mechanical synchronization between ADV and video observations. During the experiments, the onset of sediment motion was associated to the passage of the leading edge of the positive surge, and a transient sheet flow motion was observed afterward, short-lived and intense. The sediment particles were subjected to large horizontal accelerations, with a sizeable portion of particles being accelerated in excess of 10 m/s^2 (Fig. 4).

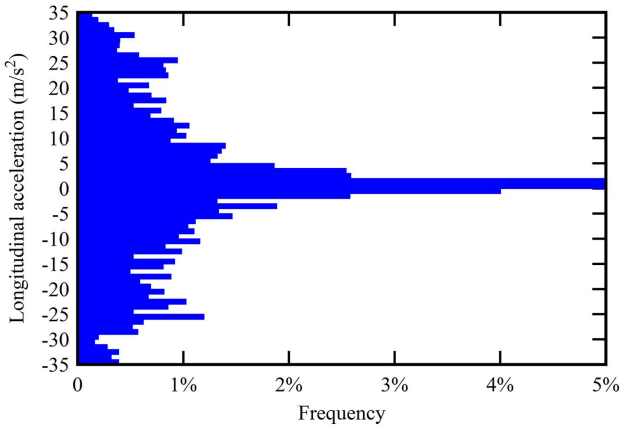

Fig. 4. Histogram of instantaneous particle accelerations beneath a breaking bore in laboratory-Natural river pebbles sieved between 6.7 mm and 9.5 mm, video observations at 1,200 fps in high-definition (Data: Li and Chanson 2018)— Flow conditions: Fr = 1.42, d_o = 0.161 m, U = 1.02 m/s, B = 0.5 m.

In the field, some acoustic Doppler velocimetry was applied to tidal bore studies (Chanson et al. 2007; Furgerot et al. 2013; Keevil et al. 2015) (Table 2). The instantaneous velocity measurements were conducted at relatively high frequencies, i.e., 50 Hz to 200 Hz, and the signals were analyzed with a Fourier decomposition technique. In addition, instantaneous suspended sediment concentration (SSC) measurements were recorded in the Garonne River tidal bore (Keevil et al. 2015; Reungoat et al. 2019). The SSC measurements relied upon a careful calibration in laboratory, typically within 48 h to 72 h from sediment sample collection. Further, a number of sediment-laden water samples were also collected during the field measurements to validate the approach (Fig. 5). The calibration of the ADV for SSC showed a massive signal attenuation for SSC > 5 to 10 kg/m^3 (Fig. 6), while the water samples collected in situ revealed SSC levels up to over 100 kg/m^3 after the tidal bore passage and typically in excess of 15 kg/m^3 during the early flood tide (Fig. 5, far right). The calibration relationships were qualitatively consistent with a number of studies with cohesive sediment materials (Ha et al. 2009; Guerrero et al. 2011; Salehi and Strom 2009, 2011; Brown and Chanson 2012). Typical granulometric observations for the Garonne River tidal bore study are presented in Fig. 7 for completeness,

A turbulent event analysis was applied to the simultaneous velocity and SSC signals in the field (Leng et al. 2018a). The results demonstrated that the turbulent bursts were responsible for major mixing and sedimentary processes. The data further showed shorter dimensionless event durations, larger event amplitudes and magnitudes beneath a tidal bore than in microtidal estuary and atmospheric boundary layer.

Velocity Profiling in Transient Free-Surface Flows

Basic Aplications

In a transient free-surface flow such as a compression wave, the experimental measurements have to be repeated to derive turbulence properties based upon an ensemble-average method. The process is onerous, repetitive and time-consuming, and it could be shortened using a fast response profiling system. Recently, laboratory experiments were performed with one or two Nortek

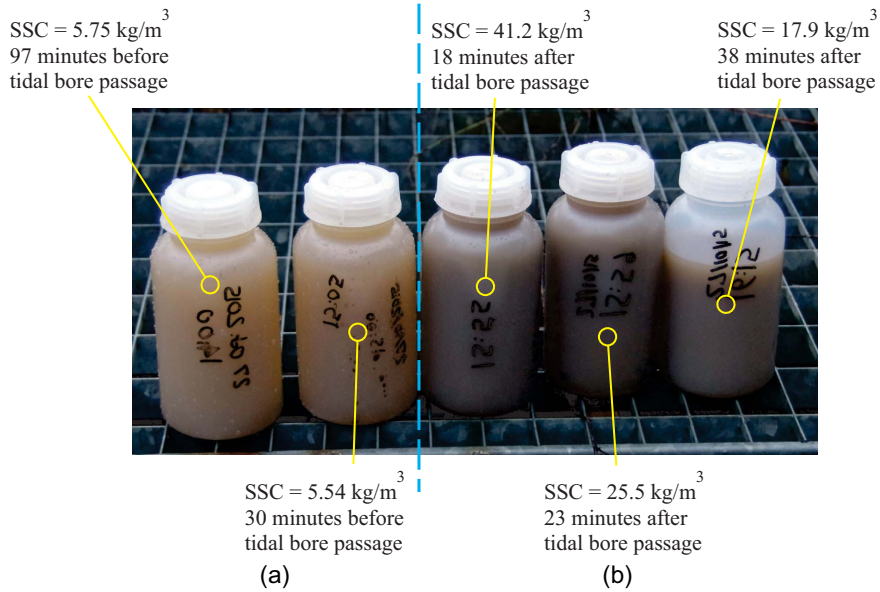

Fig. 5. Sediment-laden water samples collected before (a) and after (b) a tidal bore—Garonne River in the Arcins channel on 27 October 2015-Flow conditions: Fr = 1.33, d_o = 1.24 m, U = 4.61 m/s, B = 65.9 m.

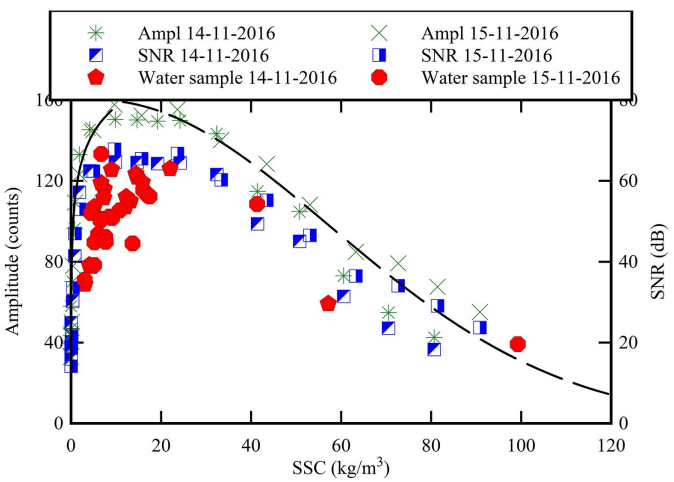

Fig. 6. Relationship between ADV signal amplitude, signal to noise ratio (SNR) and suspended sediment concentration (SSC)—Comparison with sediment-laden water samples collected in the Garonne River before and after a tidal bore on 14 and 15 November 2016 ($d_{50} \approx 17$ μm).

acoustic Doppler velocimeter Vectrino II profilers (Leng and Chanson 2017b, 2019b) (Fig. 8).

The ADV profiler was capable of recording velocity components quasi-simultaneously in a straight profile of up to 35 mm in length at relatively high frequency (100 Hz) (Dilling and Macvicar 2017; Valero and Bung 2018) (Fig. 8). The profiler outputs further enabled some advanced signal processing, including one-dimensional and two-dimensional space-time correlations (Leng and Chanson 2017a, 2019b). The turbulent integral time scales and turbulent integral length scales were derived from the cross-correlation of instantaneous velocity signals at two different locations (y_1, z_1) and (y_2, z_2) on a vertical plane:

$$R_{1,2}(\tau) = \frac{\overline{v_1(t) \times v_2(t+\tau)}}{\sqrt{v_1^2} \times \sqrt{v_2^2}} \quad (2)$$

where v is a velocity component (v = v_x, v_y or v_z) and τ is the time. The turbulent integral length scale L_T is a characteristic size of large coherent structures found in the velocity component direction:

$$L_T = \int_0^{\Delta l_{max}} (R_{1,2})_{max} \times \delta l \quad (3)$$

with δl the distance connecting the two different sampling locations [i.e., (y_1, z_1) and (y_2, z_2)], e.g., $\delta l = \delta y$ or δz for single profiler deployment depending upon the profile orientation. The turbulent integral time scale T_T characterizes the lifespan of large coherent motion detected in the velocity component:

$$T_T = \frac{1}{L_T} \times \int_0^{\Delta l_{max}} (R_{1,2})_{max} \times T_{1,2} \times \delta l \quad (4)$$

with $T_{1,2}$ the integral of cross-correlation function between the time lag associated with the peak correlation $(R_{1,2})_{max}$ and the first crossing of the cross-correlation function with zero.

In transient surges and bores, the turbulent integral time and length scales in the vertical direction were derived from the ensemble-averaged cross-correlation functions. The results presented marked differences between the initially steady flow, the short rapid deceleration phase and the early flood tide, immediately after surge passage. The laboratory data yielded integral time and length scale with an order of magnitude between 10 ms < T_T < 100 ms, and 10^{-3} m < L_T < 10^{-2} m, similar to previous laboratory and field data (Leng and Chanson 2017a, 2018, 2019b). The integral turbulent time and length scales were similar in magnitudes for the same transient flow phase. The turbulent scale data indicated that the propagation of a positive surge was an anisotropic process, with larger length scales in the transverse component, compared to the longitudinal and vertical velocity components. The turbulent length and time scales tended to increase during and after the surge passage, in comparison to those during the initially steady flows. The data suggested the presence of large vortical structures with large vertical extent, and the lifespan of turbulent structures were larger in the vertical direction compared to those in the horizontal directions.

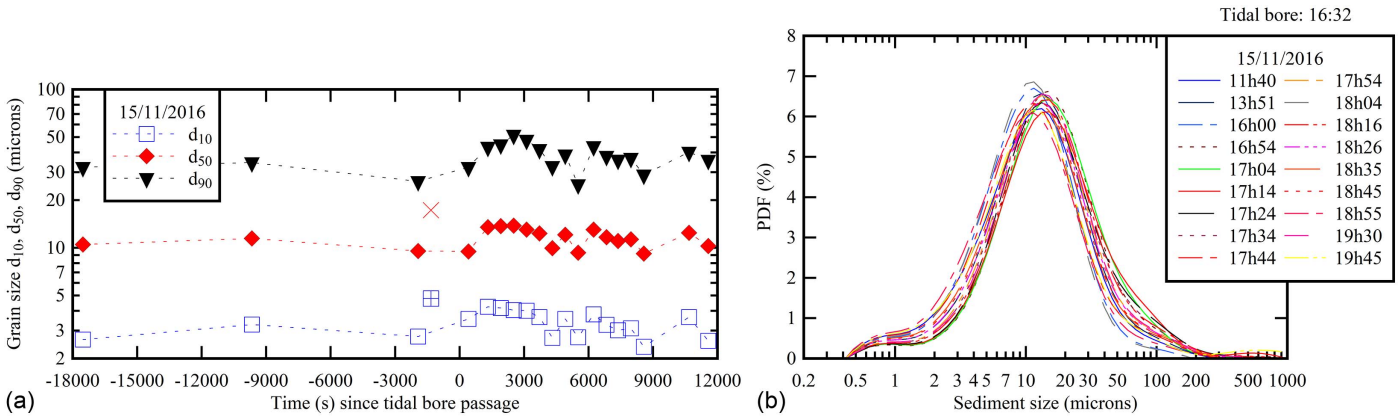

Fig. 7. Granulometric curves of sediment-laden water samples collected in the Garonne River before and after a tidal bore on 15 November 2016—Flow conditions: Fr = 1.07, d_o = 0.86 m, U = 4.26 m/s, B = 70.3 m: (a) time-variations of the characteristic grain sizes d_{10}, d_{50} and d_{90} before and after the tidal bore; and (b) grain size distributions.

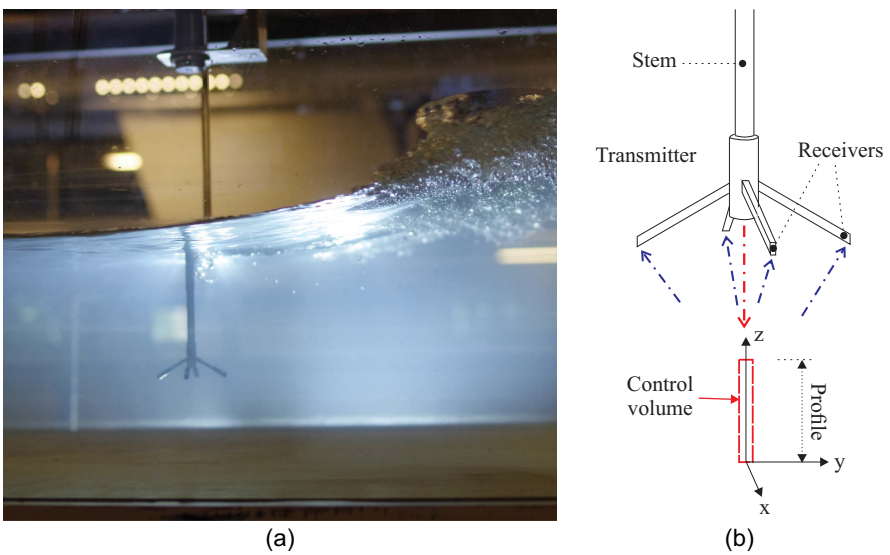

Fig. 8. Velocity profiling in a breaking bore: (a) vertical ADV profiling in an advancing breaking bore with bore direction from right to left—Flow conditions: Fr = 1.5, d_1 = 0.175 m, U = 1.3 m/s, B = 0.7 m shutter speed: 1/500 s; and (b) definition sketch of a single ADV Nortek™ Vectrino II profiler.

Practical Experience

Some instrumental errors were previously reported with the ADV profiler. (Craig et al. 2011; Zedel and Hay 2011; Macvicar et al. 2014; Leng and Chanson 2017b, 2018). In both steady and unsteady free-surface flows, the profiler tended to produce errors in terms of time-averaged velocity data and velocity fluctuations for a number of points, called weak spots, in a profile (e.g., Thomas et al. 2017; Liu et al. 2022). Even at the locations where the time-averaged velocity was meaningful, the profile of velocity fluctuations would contain errors and erroneous data.

In steady flows in a 19 m long 0.7 m wide channel, systematic tests were undertaken across the channel centreline using Vectrino II profilers mounted vertically and horizontally at different vertical elevations below the water surface. Typical results are presented in Fig. 9 and compared to ADV Vectrino+ data in the same channel for the same flow conditions. Fig. 9(a) shows the transverse profiles of the time-averaged velocity components at different vertical elevations from $z/d_1 = 0.17$ to 0.86 (present study). The ADV data was point measurements conducted on the channel centerline, whereas the Vectrino II data were profiled horizontally and centered about the centreline. The results highlighted a number of features of the side-looking profiler. The profiler seemed to estimate the transverse and vertical velocity components with better accuracy, compared to the estimation of the longitudinal velocity component, for that configuration. The longitudinal velocity was better estimated at a certain transverse range encompassing the channel centreline ($y/B = 0.490$ to 0.515) than at $0.485 < y/B < 0.49$ and $0.515 < y/B < 0.525$. The transverse profiles of the velocity fluctuations at different vertical elevations, characterized by the standard deviations v', are shown in Fig. 9(b), with comparison to the ADV data. The velocity fluctuations of the profiler data showed a curvy shape, with the higher fluctuations observed at the two ends of the profile and lower fluctuations at middle part of the profile. With increasing vertical elevations, the data quality of the longitudinal velocity fluctuation decreased, with a consistent increase in

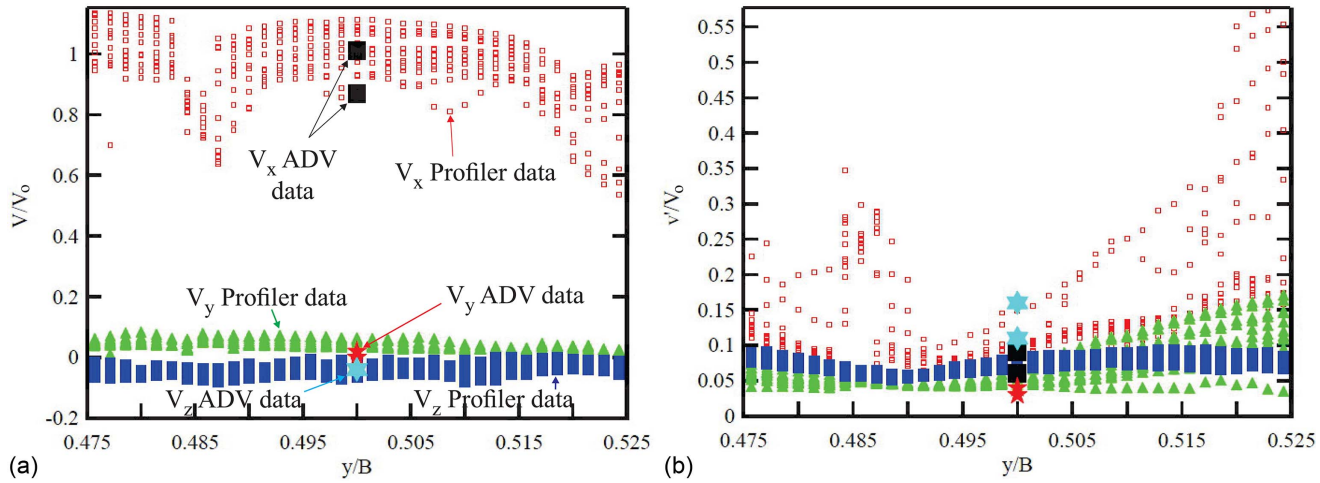

Fig. 9. Transverse profiles of time-averaged velocity components and associated fluctuations in all three directions, compared to ADV measurements for vertical elevations from 0. $15 < z/d_o < 0.86$—Sampling frequency: 100 Hz (Vectrino II profiler) and 200 Hz (Vectrino+ADV)—Steady flow conditions: $d_o = 0.174$ m, B = 0.7 m, $0.15 < z/d_o < 0.86$, $0.475 < y < B < 0.525$—Same legend for both graphs: (a) time-averaged velocity; and (b) velocity fluctuations.

standard deviation at the right end of the profile. The magnitudes of vertical velocity fluctuations with the profiler were overall lower than that of the ADV unit equipped with side-looking head. This could be due to a known limitation of ADV units, the receivers of which may be affected by the bed reflection (Finelli et al. 1999; Chanson et al. 2007).

In transient free-surface flows, the performance of ADV profiler was acceptable, subject to a careful validation for all profiler data outputs. In the authors' experience, both ADVs and ADV profilers functioned better in unsteady transient free-surface flows in laboratory, than in steady flows. In laboratory conditions, the particle count was typically low, i.e., compared to a field application, and the transient surges resuspended particles during the surge propagation, yielding a higher signal amplitude and SNR. While observed with both ADVs and ADV profilers, the effects were more beneficial to the ADV profiler signals. All in all, the velocity profiling could be a valuable technique in highly transient flows, when carefully-controlled experiments can be repeated systematically to perform ensemble-averaging. In addition, a number of additional velocity characteristics can be extracted using one or two profilers, including velocity gradient, vorticity and strain rate data (Leng and Chanson 2019b). In regions of high kinetic energy dissipation rate, some understanding of the structure and in-homogeneous turbulence in a spatially and temporally varying turbulent flow may be derived from the instantaneous velocity gradient tensor (Mckeon et al. 2007). Typical results in transient breaking surges are illustrated in Fig. 10, in which the velocity gradient tensor $\partial V_y/\partial z$ and $\partial V_z/\partial y$ and the ensemble-averaged time-variations were derived from an array of two profilers, one mounted vertically and the other horizontally. Before the surge passage, an alternating pattern between slightly positive and negative gradient values was observed in the space-time variation data set (Fig. 10). During the surge passage, the velocity gradients fluctuated rapidly throughout the transverse profile. In the wake of the surge, after its passage, the magnitudes of the velocity gradient tensor decreased. The propagation of the breaking surge caused the fluctuations in velocity gradients to decrease with time, reacting less rapidly to the bore passage, with increasing elevations.

Discussion

Practical Experience and Applications

The acoustic Doppler velocimetry evolved from the original ADV sampling at 25 Hz (Kraus et al. 1994) to more advanced instruments. Developments included a faster sampling rate up to 200 Hz, side-looking head for laboratory applications, sturdy field stem and head used in tidal bores, up to velocity profiling (Table 2). While there have been other instrumentation developments, one major benefit of acoustic Doppler velocimetry is the capability and ease to use of the same instrument in the field and in laboratory, albeit with some differences (Table 3). This was evidenced in coastal conditions (Lohrmann et al. 1995) and more recently in tidal bores in large rivers (Mouaze et al. 2010; Chanson et al. 2007; Reungoat et al. 2017). The joint usage facilitates the data analyses and the comparison between field and laboratory data, thus enabling a more accurate assessment of potential scale effects (e.g., Chanson and Toi 2015).

In steady and unsteady flows, more advanced signal decomposition techniques were applied to ADV velocity signal outputs, in particular the triple-decomposition (Table 4). In a flow motion characterized by slow-frequency fluctuations, the instantaneous time-series, e.g., of the velocity signal, may be represented as a superposition of three components:

$$V = \langle V \rangle + [V] + \{V\} \quad (5)$$

where V is the instantaneous velocity measurement, <V> the low-pass filtered contribution, [V] the band-pass filtered or slow-fluctuation component, and {V} is the high-pass filtered component corresponding to true turbulence. The triple decomposition application requires the selection of physically meaningful cutoff frequencies, F_1 and F_2, where F_1 is the upper cutoff frequency of low-pass filtered component and F_2 is the lower cutoff frequency of high-pass filtered signal. Some detailed sensitivity analyses were undertaken in a number of physical studies, in the laboratory and in the field. The findings are summarized in Table 4, including laboratory and field studies, in steady and unsteady flows. The results indicated that the mean contribution <V> was little affected by a cutoff frequency selected such as: $F_1 < 1/10 \times F_d$ to $1/3 \times F_d$,

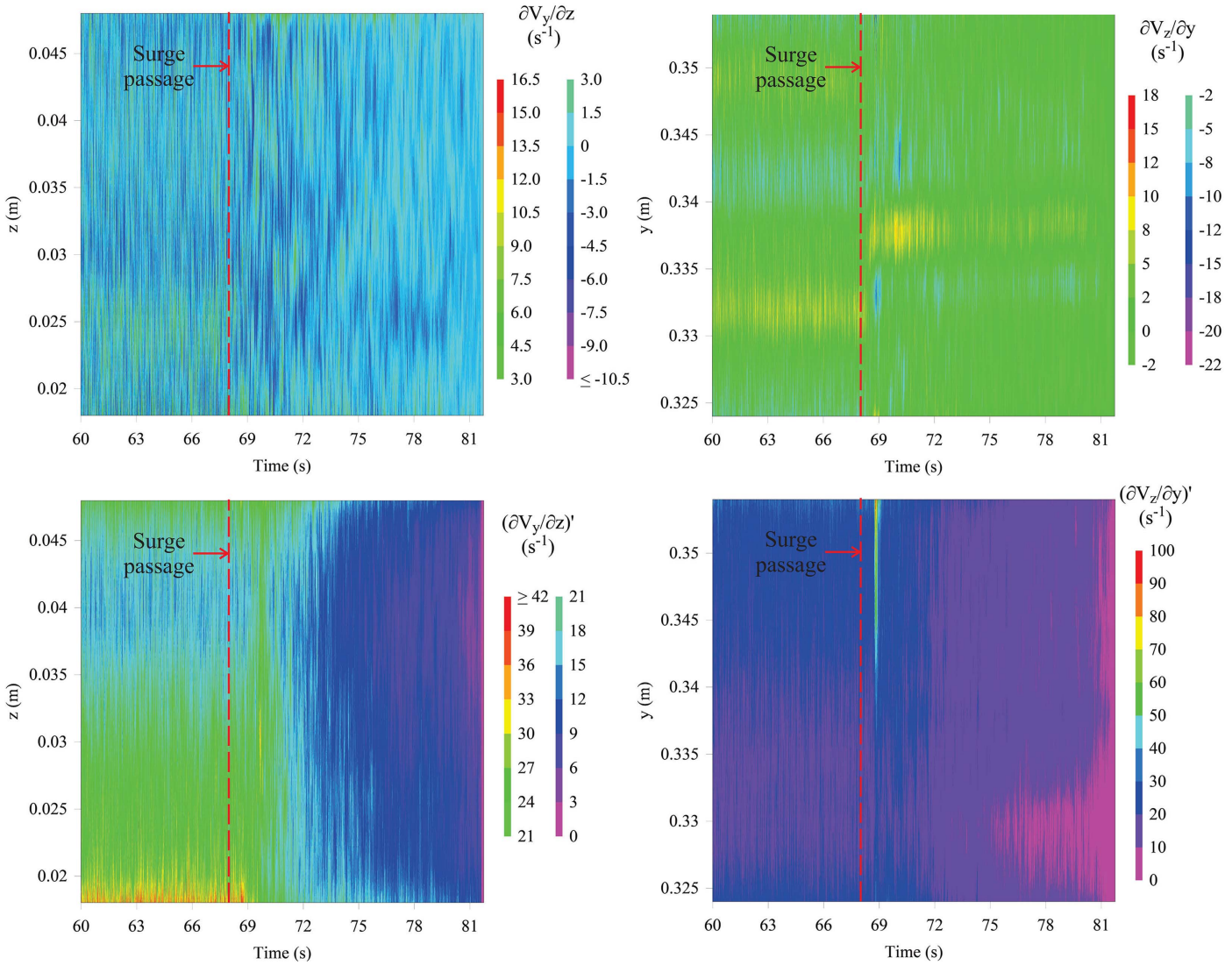

Fig. 10. Space-time contour of ensemble-averaged velocity gradient and velocity gradient fluctuations of tensor $\partial V_y/\partial z$ and $\partial V_z/\partial y$ during the propagation of a breaking bore—Flow conditions: $Fr = 1.52$, $d_o = 0.174$ m, $U = 1.3$ m/s, $B = 0.7$ m, $0.092 < z/d_o < 0.287$, $0.46 < y/B < 0.51$—Time of bore front passage: $t = 68$ s, sampling rate: 100 Hz, 25 repetitions.

Table 3. Advantages and weaknesses of field and laboratory measurements of transient free-surface flows with acoustic Doppler velocimetry

Main point	Field measurements	Laboratory measurements
Pros	Full scale/Reference	Controlled flow conditions
	Mobile bed and sedimentary processes	Repeatability
	Large number of particles in water	Ensemble statistical data set (possible)
	Same instrumentation as in laboratory study	Same instrumentation as in field study
	Fast sampling frequency	Fast sampling frequency
	Relative ease of synchronization with other instrumentation	Relative ease of synchronization with other instrumentation
Cons	Uncontrolled flow conditions	Physical limitations of laboratory and flume
	Meteorological conditions	
	Safety and dangers	Cost of construction, operation and maintenance of facility
	Point measurements	Scaled physical model and scaled hydrodynamic conditions
	Limited signal processing options	Potential scale effects in smaller models
Others	Access (often limited)	Limitations and costs of mobile bed experiments
	Observation site (limited selection)	Limited amount of particles in water
	Limited observation duration (e.g., tidal bore)	(particle seeding might be required)
	High risks of instrumentation damage and loss	

Table 4. Triple-decomposition applications with acoustic Doppler velocimetry

Reference	Flow motion	ADV	Signal sampling and processing	Dominant frequency F_d (Hz)	Lower cutoff frequency F_1 (Hz)	Upper cutoff frequency F_2 (Hz)	Comment
Fox et al. (2005)	Submerged barb obstacle	Sontek (10 MHz)	25 Hz (continuous), Moving average	1.6	—	—	Laboratory study
Trevethan and Aoki (2009)	Estuarine lake with wind waves[a]	Nortek Vector (6 MHz)	32 Hz (continuous for over 25 h), Linear filtration method	0.7–0.9	0.3	1.2	Field measurements at Hamana Lake (Japan)
Brown and Chanson (2013)	Inundated car park during major urban flooding[a]	Sontek microADV (16 MHz)	50 Hz (continuous for several hours), Fourier decomposition	0.0065–0.018	0.002	0.33	Field measurements in Brisbane River flood plain (Australia)
Hu et al. (2022)	Culvert barrel with sidewall baffles	Nortek Vectrino+ (10 MHz)	200 Hz (continuous), Fourier decomposition	0.36–0.83	$F_d/3$	$3 \times F_d$	Laboratory study

[a]Unsteady flow motion.

with F_d the dominant frequency, while the high-frequency turbulent component {V} was nearly independent of an upper cutoff frequency for $F_2 > 3 \times F_d$ to $10 \times F_d$.

The introduction of the triple decomposition processing is recommended in presence of periodic motion, which may be caused by internal resonance, sloshing between boundaries and/or wind wave motion (e.g., Trevethan and Aoki 2009; Brown and Chanson 2013). In practice, the ADV signal data must be postprocessed to remove erroneous data and spikes, before the application the triple decomposition.

On the Effects of Air Bubbles and Air Entrainment

While some early studies discussed the effects of air bubbles in ADV signals (Matos et al. 2002; Liu et al. 2002), the authors always placed the ADV probe sensors, i.e., emitter and receivers, in the water in the initially-steady flow, prior to the unsteady surge motion. During the passage of a breaking bore, in which some significant air entrainment took place (Leng and Chanson 2019a, b, c; Shi et al. 2023a, b), the ADV sensors were below the bubbly region of the roller and no adverse impact of the entrained bubbles was observed. For completeness, some preliminary tests were conducted with an ADV unit placed above the initially-steady water surface, in an attempt to characterize the turbulence in a roller. The experience demonstrated that the wetting of the probe sensors was relatively slow compared to the transient process and no physically meaningful signal data were achieved. Some coastal colleagues reported a similar experience.

Conclusion

The acoustic Doppler velocimeter (ADV) was developed about 30 years ago to perform detailed velocity measurements in free-surface flows. The metrology has been successfully used in laboratory and in the field, across a wide range of flow typology and conditions. For the last two decades, a number of successful applications were undertaken in highly transient free-surface flows, including positive and negative surges, with field applications in tidal bores of large rivers, e.g., Garonne and Sélune Rivers.

The experience and expertise in transient flows highlighted the importance of the signal processing, with a number of signal analysis methods encompassing including single realization, Fourier component method, ensemble averaging, and ensemble statistics of Fourier component analyses. In both laboratory and field works, a fine synchronization of all instrumentations is critical to the quality of the data outputs and analyses. In laboratory, the ensemble-averaging approach was most successful to characterize the transient turbulence, although it required a high degree of experimental repeatability. The ADV metrology implicitly requires an amount of water seeding, that may imply a need for artificial seeding in laboratory facilities. Alternatively, particle seeding is not an issue in the field, and the signal amplitude may be calibrated and correlated with the suspended sediment concentration (SSC), although large SSC levels may require some suitable adjustment of the ADV unit power setting. Very recent works with ADV profilers provided a wider range of turbulence characteristics in highly unsteady positive surge flow, despite the intrinsic limitations of the profiler system and the discontinued production of the Vectrino II system.

Finally, one cannot stress again the major benefit of the acoustic Doppler velocimetry for its capability and ease to use in both field and laboratory, i.e., using the same instrumentation. Both authors experienced the implicit advantage of this aspect, having been involved in physical study of and field measurements in tidal bores. The usage of the same metrology eases the data analyses and provides a greater level of confidence in the comparison between prototype and model data.

Data Availability Statement

All data or models that support the findings of this study are available from the corresponding author upon reasonable request.

Acknowledgments

The first author thanks a large number of colleagues and former students who assisted with the field and laboratory work, in particular Dr. Jan Becker, Dr. Youkai Li, Dr. Nazanin Khezri, Christian Koch, Prof. Pierre Lubin, Dr. Bruce Macvicar, Prof. Colin Rennie, Dr. Martina Reichstetter, Dr. David Reungoat, Dr. Rui (Ray) Shi, Dr. Bruno Simon, Dr. Hang Wang, Dr. Gangfu Zhang (in alphabetical order). Both authors further acknowledge the technical assistance of Jason van der Gevel and Stewart Matthews (The University of Queensland). The two anonymous reviewers are thanked for their pertinent comments. The following financial support is acknowledged: the Australian Research Council, Australia (Grants LP0347242, LP110100431, DP120100481, LP140100225, DP190103379), Agence Nationale de la Recherche (France) (Grant ANR MASCARET ANR-10-BLAN-0911), QLD Department of

Transport and Main Roads (Grant TMTHF1805), Apiary Financial (Grantor RE333704).

Notation

The following symbols are used in this paper:

B = channel width (m);
d = water depth (m) measured normal to the invert;
d_o = initial water depth (m);
d_{10} = first decile of sediment grain size distribution (m);
d_{50} = median sediment grain size (m);
d_{90} = ninth decile of sediment grain size distribution (m);
F_c = threshold frequency (Hz);
F_d = dominant frequency (Hz) of slow-frequency fluctuations;
F_1 = lower cutoff frequency (Hz);
F_3 = upper cutoff frequency (Hz);
Fr = Froude number of transient surge;
L = channel test section length (m);
L_T = integral turbulent length scale (m);
n = number of receivers;
R = normalized cross-correlation coefficient;
SNR = signal to noise ratio (dB);
SSC = suspended sediment concentration (kg/m^3);
T_T = integral turbulent time scale (s);
t = time (s);
U = surge celerity (m/s);
V = velocity (m/s);
$\langle V \rangle$ = low-pass filtered velocity component (m/s);
$[V]$ = band-pass filtered velocity component (m/s);
$\{V\}$ = high-pass filtered velocity component (m/s);
V_i = initial flow velocity (m/s);
V_x = longitudinal velocity component (m/s) positive downstream;
V_y = transverse velocity component (m/s);
V_z = vertical velocity component (m/s) positive upward;
v = instantaneous velocity fluctuation (m/s);
v_x = instantaneous longitudinal velocity fluctuation (m/s);
v_y = instantaneous transverse velocity fluctuation (m/s);
v_z = instantaneous vertical velocity fluctuation (m/s); and
τ = time lag (s).

Subscripts

i = x, y or z;
o = initial flow conditions;
x = longitudinal component;
y = transverse component; and
z = vertical component.

References

Aleixo, R., S. Soares-Frazao, and Y. Zech. 2019. "Statistical analysis methods for transient flows—The dam-break case." *J. Hydraul. Res.* 57 (5): 688–701. https://doi.org/10.1080/00221686.2018.1516700.

Bradshaw, P. 1971. *An introduction to turbulence and its measurement*. Oxford, UK: Pergamon Press.

Brown, R., and H. Chanson. 2012. "Suspended sediment properties and suspended sediment flux estimates in an urban environment during a major flood event." *Water Resour. Res.* 48 (15): W11523. https://doi.org/10.1029/2012WR012381.

Brown, R., and H. Chanson. 2013. "Turbulence and suspended sediment measurements in an urban environment during the Brisbane river flood of January 2011." *J. Hydraul. Eng.* 139 (2): 244–252. https://doi.org/10.1061/(ASCE)HY.1943-7900.0000666.

Chanson, H. 2020. "Statistical analysis method for transient flows—The dam-break case. Discussion." *J. Hydraul. Res.* 58 (6): 1001–1004. https://doi.org/10.1080/00221686.2020.1729266.

Chanson, H., and N. J. Docherty. 2012. "Turbulent velocity measurements in open channel bores." *Eur. J. Mech. Fluids* 32 (Mar): 52–58. https://doi.org/10.1016/j.euromechflu.2011.10.001.

Chanson, H., P. Lubin, B. Simon, and D. Reungoat. 2010. *Turbulence and sediment processes in the tidal bore of the Garonne River: First observations*. Rep. No. CH79/10. Brisbane, QLD, Australia: Univ. of Queensland.

Chanson, H., D. Reungoat, B. Simon, and P. Lubin. 2011. "High-frequency turbulence and suspended sediment concentration measurements in the Garonne River tidal bore." *Estuarine Coastal Shelf Sci.* 95 (2–3): 298–306. https://doi.org/10.1016/j.ecss.2011.09.012.

Chanson, H., M. Takeuchi, and M. Trevethan. 2008. "Using turbidity and acoustic backscatter intensity as surrogate measures of suspended sediment concentration in a small sub-tropical estuary." *J. Environ. Manage.* 88 (4): 1406–1416. https://doi.org/10.1016/j.jenvman.2007.07.009.

Chanson, H., and Y. H. Toi. 2015. "Physical modelling of breaking tidal bores: Comparison with prototype data." *J. Hydraul. Res.* 53 (2): 264–273. https://doi.org/10.1080/00221686.2014.989458.

Chanson, H., M. Trevethan, and C. Koch. 2007. "Turbulence measurements with acoustic doppler velocimeters. Discussion." *J. Hydraul. Eng.* 133 (11): 1283–1286. https://doi.org/10.1061/(ASCE)0733-9429(2005)131:12(1062).

Craig, R. G. A., C. Loadman, B. Clement, P. J. Ruesello, and E. Siegel. 2011. "Characterization and testing of a new bistatic profiling acoustic doppler velocimeter: The Vectrino-II." In *Proc., IEEE/OES/CWTM 10th Working Conf. on Current, Waves and Turbulence Measurement*, 246–252. New York: IEEE Oceanic Engineering Society.

Dilling, S., and B. J. Macvicar. 2017. "Cleaning high-frequency velocity profile data with autoregressive moving average (ARMA) models." *Flow Meas. Instrum.* 54 (Apr): 68–81. https://doi.org/10.1016/j.flowmeasinst.2016.12.005.

Finelli, C. M., D. D. Hart, and D. M. Fonseca. 1999. "Evaluating the spatial resolution of an acoustic doppler velocimeter and the consequences for measuring near-bed flows." *Limnol. Oceanogr.* 44 (7): 1793–1801. https://doi.org/10.4319/lo.1999.44.7.1793.

Fischer, H. B., E. J. List, R. C. Y. Koh, J. Imberger, and N. H. Brooks. 1979. "Academic." In *Mixing in inland and coastal waters*. New York: Academic Press.

Fox, J. F., A. N. Papanicolaou, and L. Kios. 2005. "Eddy taxonomy methodology around submerged barb obstacle within a fixed rough bed." *J. Eng. Mech.* 131 (10): 1082–1101. https://doi.org/10.1061/(ASCE)0733-9399(2005)131:10(1082).

Fugate, D. C., and C. T. Friedrichs. 2002. "Determining concentration and fall velocity of estuarine particle populations using Adv, OBS and LISST." *Cont. Shelf Res.* 22 (11–13): 1867–1886. https://doi.org/10.1016/S0278-4343(02)00043-2.

Furgerot, L., D. Mouaze, B. Tessier, L. Perez, and S. Haquin. 2013. "Suspended sediment concentration in relation to the passage of a tidal bore (Sée River Estuary, Mont Saint Michel, NW France)." In *Proc., Coastal Dynamics 2013*, 671–682. Bordeaux, France: Univ. of Bordeaux, the Centre National de la Recherche Scientifique.

Goring, D. G., and V. I. Nikora. 2002. "Despiking acoustic doppler velocimeter data." *J. Hydraul. Eng.* 128 (1): 117–126. https://doi.org/10.1061/(ASCE)0733-9429(2002)128:1(117).

Guerrero, M., R. N. Szupiany, and M. Amsler. 2011. "Comparison of acoustic backscattering techniques for suspended sediments investigation." *Flow Meas. Instrum.* 22 (5): 392–401. https://doi.org/10.1016/j.flowmeasinst.2011.06.003.

Ha, H. K., W. Y. Hsu, J. P. Y. Maa, Y. Y. Shao, and C. W. Holland. 2009. "Using ADV backscatter strength for measuring suspended cohesive sediment concentration." *Cont. Shelf Res.* 29 (10): 1310–1316. https://doi.org/10.1016/j.csr.2009.03.001.

Halfi, E., D. Paz, K. Stark, U. Yogev, I. Reid, M. Dorman, and J. B. Laronne. 2020. "Novel mass-aggregation-based calibration of an acoustic method of monitoring bedload flux by infrequent desert flash floods." *Earth Surf. Process. Landf.* 45 (14): 3510–3524. https://doi.org/10.1002/esp.4988.

Halfi, E., S. K. Thappeta, J. P. L. Johnson, I. Reid, and J. B. Laronne. 2023. "Transient bedload transport during flashflood bores in a desert gravel-bed channel." *Water Resour. Res.* 59 (17): e2022WR033754. https://doi.org/10.1029/2022WR033754.

Hinze, J. O. 1975. *Turbulence*. 2nd ed. New York: McGraw-Hill.

Hornung, H. G., C. Willert, and S. Turner. 1995. "The flow field downstream of a hydraulic jump." *J. Fluid Mech.* 287 (Aug): 299–316. https://doi.org/10.1017/S0022112095000966.

Hu, J., Y. Li, and H. Chanson. 2022. "Near-full-scale physical modelling and open-channel flow velocity in a fish-friendly culvert with full-height sidewall baffles." In *Proc., 9th IAHR Int. Symp. on Hydraulic Structures*. Logan, UT: Utah State Univ.

Karlsson, R. I., and T. G. Johansson. 1986. "LDV measurements of higher order moments of velocity fluctuations in a turbulent boundary layer." In *Proc., 3rd Int. Symp. on Applications of Laser Anemometry to Fluid Mechanics*. Lisbon, Portugal: Instituto Superior Técnico.

Keevil, C. E., H. Chanson, and D. Reungoat. 2015. "Fluid flow and sediment entrainment in the Garonne river bore and tidal bore collision." *Earth Surf. Process. Landf.* 40 (12): 1574–1586. https://doi.org/10.1002/esp.3735.

Khezri, N., and H. Chanson. 2012. "Inception of bed load motion beneath a bore." *Geomorphology* 153-154 (Jun): 39–47. https://doi.org/10.1016/j.geomorph.2012.02.006.

Koch, C., and H. Chanson. 2008. "Turbulent mixing beneath an undular bore front." *J. Coast. Res.* 244 (4): 999–1007. https://doi.org/10.2112/06-0688.1.

Kraus, N. C., A. Lohrmann, and R. Cabrera. 1994. "New acoustic meter for measuring 3D laboratory flows." *J. Hydraul. Eng.* 120 (3): 406–412. https://doi.org/10.1061/(ASCE)0733-9429(1994)120:3(406).

Krogstad, P. A., H. I. Andersson, O. M. Bakken, and A. A. Ashrafian. 2005. "An experimental and numerical study of channel flow with rough walls." *J. Fluid Mech.* 530 (May): 327–352. https://doi.org/10.1017/S0022112005003824.

Leng, X. 2018. "A study of turbulence: The unsteady propagation of bores and surges." Ph.D. thesis, School of Civil Engineering, Univ. of Queensland.

Leng, X., and H. Chanson. 2015. "Unsteady turbulence in expansion waves in rivers and estuaries: An experimental study." *Environ. Fluid Mech.* 15 (5): 905–922. https://doi.org/10.1007/s10652-014-9385-9.

Leng, X., and H. Chanson. 2016. "Coupling between free-surface fluctuations, velocity fluctuations and turbulent Reynolds stresses during the upstream propagation of positive surges, bores and compression waves." *Environ. Fluid Mech.* 16 (4): 695–719. https://doi.org/10.1007/s10652-015-9438-8.

Leng, X., and H. Chanson. 2017a. "Unsteady turbulence, dynamic similarity and scale effects in bores and positive surges." *Eur. J. Mech.* 61 (Aug): 125–134. https://doi.org/10.1016/j.euromechflu.2016.09.017.

Leng, X., and H. Chanson. 2017b. "Unsteady velocity profiling in bores and positive surges." *Flow Meas. Instrum.* 54 (Apr): 136–145. https://doi.org/10.1016/j.flowmeasinst.2017.01.004.

Leng, X., and H. Chanson. 2018. "Transverse velocity profiling under positive surges in channels." *Flow Meas. Instrum.* 64 (Dec): 14–27. https://doi.org/10.1016/j.flowmeasinst.2018.10.006.

Leng, X., and H. Chanson. 2019a. "Air-water interaction and characteristics in breaking bores." *Int. J. Multiphase Flow* 120 (17): 103101. https://doi.org/10.1016/j.ijmultiphaseflow.2019.103101.

Leng, X., and H. Chanson. 2019b. "Two-dimensional integral turbulent scales in compression wave in a canal." *Exp. Therm Fluid Sci.* 102 (Apr): 163–180. https://doi.org/10.1016/j.expthermflusci.2018.09.014.

Leng, X., and H. Chanson. 2019c. "Two-phase flow measurements of an unsteady breaking bore." *Exp. Fluids* 60 (3): 1–15. https://doi.org/10.1007/s00348-019-2689-2.

Leng, X., H. Chanson, and D. Reungoat. 2018a. "Turbulence and turbulent flux events in tidal bores: Case study of the undular tidal bore of the Garonne River." *Environ. Fluid Mech.* 18 (4): 807–828. https://doi.org/10.1007/s10652-017-9561-9.

Leng, X., B. Simon, N. Khezri, P. Lubin, and H. Chanson. 2018b. "CFD modelling of tidal bores: Development and validation challenges." *Coastal Eng. J.* 60 (4): 423–436. https://doi.org/10.1080/21664250.2018.1498211.

Li, Y. 2020. "Hydrodynamics of tidal bores: Turbulent propagation and sediment transport." Ph.D. thesis, Univ. of Queensland, School of Civil Engineering.

Li, Y., and H. Chanson. 2018. "Sediment motion beneath surges and bores." In *Proc., 6th IAHR Int. Symp. on Hydraulic Structures ISHS 2018*. Logan, UT: Utah State Univ.

Liu, D., K. Alobaidi, and M. Valkyrakis. 2022. "The assessment of an acoustic Doppler velocimetry profiler from a user's perspective." *Acta Geophys.* 70 (5): 2297–2310. https://doi.org/10.1007/s11600-022-00896-3.

Liu, M., D. Zhu, and N. Rajaratnam. 2002. "Evaluation of ADV measurements in bubbly two-phase flows." In *Proc., Conf. on Hydraulic Measurements and Experimental Methods*. Reston, VA: ASCE.

Lohrmann, A., R. Cabrera, G. Gelfenbaum, and J. Haines. 1995. "Direct measurements of Reynolds stress with an acoustic doppler velocimeter." In *Proc., IEEE 5th Working Conf. on Current Measurement*, 205–210. New York: IEEE.

Lohrmann, A., R. Cabrera, and N. C. Kraus. 1994. "Acoustic-doppler velocimeter (ADV) for laboratory use." In *Proc., Conf. Fundamentals and Advancements in Hydraulic Measurements and Experimentation*. Reston, VA: ASCE.

Macvicar, B., S. Dilling, J. Lacey, and K. Hipel. 2014. "A quality analysis of the Vectrino II instrument using a new open-source MATLAB toolbox and 2D ARMA models to detect and replace spikes." In *Proc., 7th Int. Conf. on Fluvial Hydraulics (River Flow)*. Lausanne, Switzerland: Ecole Polytechnique Federale Lausanne.

Matos, J., K. H. Frizell, S. Andre, and K. W. Frizell. 2002. "On the performance of velocity measurement techniques in air-water flows." In *Proc., Conf. on Hydraulic Measurements and Experimental Methods*. Reston, VA: ASCE.

Mckeon, B. J., et al. 2007. "Nondimensional representation of the boundary-value problem." In *Experimental fluid mechanics*, 33–83. Berlin: Springer.

Mclelland, S. J., and A. P. Nicholas. 2000. "A new method for evaluating errors in high-frequency ADV measurements." *Hydrol. Process.* 14 (2): 351–366. https://doi.org/10.1002/(SICI)1099-1085(20000215)14:2<351::AID-HYP963>3.0.CO;2-K.

Mori, N., T. Suzuki, and S. Kakuno. 2007. "Noise of acoustic doppler velocimeter data in bubbly flows." *J. Eng. Mech.* 133 (1): 122–125. https://doi.org/10.1061/(ASCE)0733-9399(2007)133:1(122).

Mouaze, D., H. Chanson, and B. Simon. 2010. *Field measurements in the tidal bore of the Sélune River in the Bay of Mont Saint Michel (September 2010)*. Rep. No. CH81/10. Brisbane, QLD, Australia: Univ. of Queensland.

Nielsen, P. 1992. "Coastal bottom boundary layers and sediment transport." In *Advanced series on ocean engineering*. Singapore: World Scientific.

Nikora, V. I., and D. G. Goring. 1998. "ADV measurements of turbulence: Can we improve their interpretation?" *J. Hydraul. Eng.* 124 (6): 630–634. https://doi.org/10.1061/(ASCE)0733-9429(1998)124:6(630).

Nikora, V. I., and D. G. Goring. 2000. "Flow turbulence over fixed and weakly mobile gravel beds." *J. Hydraul. Eng.* 126 (9): 679–690. https://doi.org/10.1061/(ASCE)0733-9429(2000)126:9(679).

Perry, A. E., T. T. Lim, and M. S. Chong. 1980. "The instantaneous velocity fields of coherent structures in coflowing jets and wakes." *J. Fluid Mech.* 101 (2): 243–256. https://doi.org/10.1017/S0022112080001644.

Rajaie, M., A. Azimi, I. Nistor, and C. D. Rennie. 2022. "Experimental investigations on hydrodynamic characteristics of tsunami-like hydraulic bores impacting a square structure." *J. Hydraul. Eng.* 148 (3): 04021061. https://doi.org/10.1061/(ASCE)HY.1943-7900.0001965.

Reichstetter, M. 2011. "Hydraulic modelling of unsteady open channel flow: Physical and analytical validation of numerical models of positive and negative surges." Ph.D. thesis, School of Civil Engineering, Univ. of Queensland.

Reungoat, D., X. Leng, and H. Chanson. 2017. "Successive impact of tidal bores on sedimentary processes: Arcins channel, Garonne River." *Estuarine Coastal Shelf Sci.* 188 (Jun): 163–173. https://doi.org/10.1016/j.ecss.2017.02.025.

Reungoat, D., X. Leng, and H. Chanson. 2019. "Turbulence and Suspended Sediment Processes in the Garonne River Tidal Bore in November 2016." *Int. J. Sediment Res.* 34 (5): 496–508. https://doi.org/10.1016/j.ijsrc.2019.03.003.

Reungoat, D., P. Lubin, X. Leng, and H. Chanson. 2018. "Tidal bore hydrodynamics and sediment processes: 2010-2016 field observations in France." *Coastal Eng. J.* 60 (4): 484–498. https://doi.org/10.1080/21664250.2018.1529265.

Rutherford, J. C. 1994. *River mixing*, 347. New York: Wiley.

Salehi, M., and K. Strom. 2011. "Using velocimeter signal to noise ratio as a surrogate measure of suspended mud concentration." *Cont. Shelf Res.* 31 (9): 1020–1032. https://doi.org/10.1016/j.csr.2011.03.008.

Salehi, M., and K. B. Strom. 2009. "Suspended sediment concentration measurements of muddy sediments with an ADV." In *Proc., ASCE/EWRI World Water and Environmental Resources Congress*. Reston, VA: ASCE.

Shi, R., X. Leng, and H. Chanson. 2020. "On turbulence and turbulent events in a breaking bore." *Mech. Res. Commun.* 104 (Sep): 103478. https://doi.org/10.1016/j.mechrescom.2020.103478.

Shi, R., D. Wüthrich, and H. Chanson. 2023a. "Air-water properties of unsteady breaking bores Part 1: Novel Eulerian and Lagrangian velocity measurements using intrusive and non-intrusive techniques." *Int. J. Multiphase Flow* 159 (Feb): 104338. https://doi.org/10.1016/j.ijmultiphaseflow.2022.104338.

Shi, R., D. Wüthrich, and H. Chanson. 2023b. "Air-water properties of unsteady breaking bore Part 2: Void fraction and bubble statistics." *Int. J. Multiphase Flow* 159 (Feb): 104337. https://doi.org/10.1016/j.ijmultiphaseflow.2022.104337.

Spinewine, B. 2005. "Two-layer flow behaviour and the effects of granular dilatancy in dam-break induced sheet-flow." Ph.D. thesis, Université catholique de Louvain, Faculty of Applied Sciences.

Thomas, L., and L. David. 2022. "Eulerian and Lagrangian coherent structures in a positive surge." *Exp. Fluids* 63 (2): 43. https://doi.org/10.1007/s00348-022-03383-z.

Thomas, R. E., L. Schindfessel, S. J. Mclelland, S. Creelle, and D. E. Mulder. 2017. "Bias in mean velocities and noise in variances and covariances measured using a multistatic acoustic profiler: The Nortek Vectrino profiler." *Meas. Sci. Technol.* 28 (Jun): 075302. https://doi.org/10.1088/1361-6501/aa7273.

Trevethan, M., and S. Aoki. 2009. "Initial observations on relationship between turbulence and suspended sediment properties at Hamana Lake Japan." *J. Coast. Res.* I56 (Sep): 1434–1438.

Valero, D., and D. B. Bung. 2018. "Vectrino profiler spatial filtering for shear flows based on the mean velocity gradient equation." *J. Hydraul. Eng.* 144 (7): 04018037. https://doi.org/10.1061/(ASCE)HY.1943-7900.0001485.

Voulgaris, G., and J. H. Trowbridge. 1998. "Evaluation of the acoustic doppler velocimeter (ADV) for turbulence measurements." *J. Atmos. Oceanic Tech.* 15 (2): 272–289. https://doi.org/10.1175/1520-0426(1998)015<0272:EOTADV>2.0.CO;2.

Wahl, T. L. 2003. "Despiking acoustic doppler velocimeter data. Discussion." *J. Hydraul. Eng.* 129 (6): 484–487. https://doi.org/10.1061/(ASCE)0733-9429(2003)129:6(484).

Wang, H., X. Leng, and H. Chanson. 2017. "Bores and hydraulic jumps. Environmental and geophysical applications." *Eng. Comput. Mech.* 170 (1): 25–42. https://doi.org/10.1680/jencm.16.00025.

Wűthrich, D., M. Pfister, D. E. Cesare, and A. J. Schleiss. 2016. "Velocity profile measurements in bore waves." In *Proc., 10th Int. Symp. on Ultrasonic Doppler Methods for Fluid Mechanics and Fluid Engineering*. Tokyo: Tokyo Institute of Technology.

Zedel, L., and A. Hay. 2011. "Turbulence measurements in a jet: Comparing the Vectrino and Vectrino II." In *Proc., IEEE/OES/CWTM 10th Working Conf. on Current, Waves and Turbulence Measurements*. New York: IEEE.

Zhang, Z., C. Pan, J. Zeng, F. Chen, H. Qin, K. He, K. Zhu, and E. Zhao. 2022. "Hydrodynamics of tidal bore overflow on the spur dike and its influence on the local scour." *Ocean Eng.* 266 (13): 113140. https://doi.org/10.1016/j.oceaneng.2022.113140.